JACC: CARDIOVASCULAR IMAGING VOL. ■, NO. ■, 2019

PUBLISHED BY ELSEVIER

ORIGINAL RESEARCH

Relative Contribution of Afterload and Interstitial Fibrosis to Myocardial Function in Severe Aortic Stenosis

Alisson Slimani, MD,[a,c] Julie Melchior, MD,[a,c] Christophe de Meester, PhD,[a,c] Sophie Pierard, MD, PhD,[a,c] Clotilde Roy, MD,[a,c] Mihaela Amzulescu, MD, PhD,[a,c] Caroline Bouzin, PhD,[b] Frédéric Maes, MD,[a,c] Agnès Pasquet, MD, PhD,[a,c] Anne-Catherine Pouleur, MD, PhD,[a,c] David Vancraeynest, MD, PhD,[a,c] Bernhard Gerber, MD, PhD,[a,c] Gebrine El Khoury, MD,[a,d] Jean-Louis Vanoverschelde, MD, PhD[a,c]

ABSTRACT

OBJECTIVES The present study aimed at investigating the respective contribution of afterload and myocardial fibrosis to pre- and post-operative left ventricular (LV) function by using stress–strain relationships.

BACKGROUND Separating the effect of myocardial dysfunction and afterload on pump performance has important implications for the prognosis and management of patients with severe aortic stenosis (AS).

METHODS A total of 101 patients with isolated severe AS (57% men; mean age 71 years) and 75 healthy control subjects underwent resting 2-dimensional and speckle-tracking echocardiography to measure global circumferential strain (GCS) and global longitudinal strain (GLS), as well as end-systolic wall stress (ESWS). Normal stress–strain relationships were constructed using control subjects' data and fitted to linear regression. End-systolic stress–strain indexes (the number of SDs from the mean regression line) were used as an afterload-independent index of myocardial function and compared with myocardial fibrosis, measured on transmural myocardial biopsies harvested at the time of surgery.

RESULTS GCS and GLS were afterload-dependent in both control subjects and patients. The GLS-ESWS relationship of patients was shifted downward compared with control subjects. Patients with reduced pre-operative end-systolic stress–strain indexes exhibited larger degrees of interstitial myocardial fibrosis than patients without ($3.8 \pm 2.9\%$ vs. $8.3 \pm 6.3\%$, $p < 0.001$; and $4.9 \pm 4.4\%$ vs. $9.5 \pm 6.4\%$; $p < 0.001$, for GLS and GCS, respectively). By multivariate analysis, pre-operative end-systolic stress–strain indexes were the only predictors of post-operative longitudinal and circumferential end-systolic stress–strain indexes ($ß = 0.49$ and $ß = 0.60$, respectively; $p < 0.001$).

CONCLUSIONS Myocardial strains are afterload-dependent. In patients with severe AS, pre-operative stress–strain indexes allow identification of patients with increased myocardial fibrosis and predict the extent of functional recovery after aortic valve replacement. (J Am Coll Cardiol Img 2019;■:■–■) © 2019 by the American College of Cardiology Foundation.

In patients with valvular heart diseases, understanding the complex interplay between loading conditions and left ventricular (LV) ejection phase indexes, such as left ventricular ejection fraction (LVEF) or LV systolic strain, is crucial to deciding on the appropriate timing of surgery (1,2). This is particularly true in patients with severe aortic stenosis (AS), who had the development of concentric

From the [a]Pôle de Recherche Cardiovasculaire, Institut de Recherche Expérimentale et Clinique, Université Catholique de Louvain, Brussels, Belgium; [b]IREC Imaging Platform, Institut de Recherche Expérimentale et Clinique, Université Catholique de Louvain, Brussels, Belgium; [c]Division of Cardiology, Cliniques Universitaires Saint-Luc, Brussels, Belgium; and the [d]Division of Cardiothoracic Surgery, Cliniques Universitaires Saint-Luc, Brussels, Belgium. The authors have reported that they have no relationships relevant to the contents of this paper to disclose.

Manuscript received November 25, 2018; revised manuscript received April 26, 2019, accepted May 2, 2019.

ISSN 1936-878X/$36.00 https://doi.org/10.1016/j.jcmg.2019.05.020

ABBREVIATIONS AND ACRONYMS

AS = aortic stenosis

AVA = aortic valve area

AVR = aortic valve replacement

ESPWTh = end-systolic posterior wall thickness

ESWS = end-systolic wall stress

GSC = global circumferential strain

GLS = global longitudinal strain

LV = left ventricular

LVEF = left ventricular ejection fraction

LVESD = left ventricular end-systolic dimensions

LVESP = left ventricular end-systolic pressure

LVPSP = left ventricular peak systolic pressure

NYHA = New York Heart Association

LV hypertrophy helps to maintain LVEF within normal limits, because the increase in systolic wall thickness counteracts the effects of increased systolic pressure on systolic wall stresses (3). However, with further progression of AS, LVEF can eventually deteriorate, resulting in hemodynamic decompensation and heart failure symptoms (4). Because in many patients with severe AS and reduced LVEF, the surgical relief of LV obstruction permits LVEF to almost completely recover, it has been suggested that afterload mismatch, due to inadequate LV hypertrophy, rather than depressed contractility, is responsible for their reduction in LVEF (1,5). Yet, not every patient with severe AS and reduced LVEF has normal LVEF after aortic valve replacement (AVR) (6). In the patients who do not, persistently depressed LVEF despite successful AVR has been attributed to a self-perpetuating process of myocyte degeneration, cell death, and replacement fibrosis, which incompletely regresses upon correction of excessive afterload (7,8).

Because separating the effect of depressed myocardial contractility from that of afterload on LV ejection phase indexes has important implications for the prognosis and management of patients with severe AS (1,2), the aim of the present study was to investigate the respective contribution of excessive afterload and interstitial myocardial fibrosis to pre- and post-operative LV systolic strain. This study also determines if adjusting pre-operative strain for afterload allows identification of patients with persistent post-operative dysfunction. To achieve this, we constructed end-systolic stress–strain relationships and obtained transmural biopsies in 101 patients with severe AS who underwent AVR.

METHODS

STUDY POPULATION. The study population consisted of 101 consecutive patients with severe AS, defined by an aortic valve area (AVA) <1 cm^2 and an indexed AVA ≤ 0.6 cm^2/m^2, who were prospectively recruited between January 2015 and March 2017. All patients had a class 1 indication for AVR according to the 2012 European Society of Cardiology guidelines (9). Patients with at least moderate aortic regurgitation or mitral valve disease, a history of heart valve surgery, significant coronary artery disease (defined as previous myocardial infarction, coronary stenosis >50% at pre-operative coronary angiography), or poor echocardiographic windows were not considered for inclusion into the study. The international review board of our institution approved the study protocol. Written informed consent was obtained from all patients.

Seventy-five healthy volunteers were recruited by advertisement in the local community to construct normal end-systolic stress–strain relationships. All were considered to be normal by history, physical examination, 2-dimensional and Doppler echocardiography, as well as resting and exercise electrocardiograms. None of the subjects was taking cardiovascular drugs at the time of the study, and all were in sinus rhythm.

DOPPLER ECHOCARDIOGRAPHY. Echocardiographic data were obtained using an IE33 echocardiographic system (Philips Medical Systems, Andover, Massachusetts) equipped with a X5-1 1/5-MHz phased-array transducer. All subjects underwent a comprehensive resting examination, including 2-dimensional echocardiography and Doppler examinations. All tests were conducted by experienced cardiologists.

DATA ANALYSIS. The AVA was calculated using the continuity equation, as previously recommended (10). Mean transvalvular flow rates were calculated by dividing stroke volume by the LV ejection time. LV volumes and LVEF were calculated using the biplane Simpson method, whereas LV mass was calculated according to the method by Devereux et al. (11).

Myocardial strain was computed on 2-dimensional, gray-scale harmonic images acquired in the 3 standard apical views (2-, 3-, and 4-chamber) and the left parasternal short-axis view (at mid-ventricular level) at a frame rate of 55 to 60 frames/s during breath-hold (3 heartbeats each). Care was taken to avoid foreshortening in apical views. Native 2-dimensional images were stored digitally for later off-line analysis.

Global longitudinal strain (GLS) and global circumferential strain (GSC) were computed using a dedicated strain analysis software (Tomtec, Philips Medical Systems, Andover, Massachusetts). Briefly, for determination of GLS, markers were placed onto the mitral annulus and the apex on end-diastolic 4-chamber, 2-chamber, and long-axis apical images. For determination of GCS, markers were placed onto the endocardial borders of the 2 papillary muscles, as well as on the endocardial border of the inferior wall on end-diastolic mid-ventricular short-axis images. The software program automatically detects the endocardial contours on a frame-by-frame basis and generates deformation curves. GLS was computed as the mean of 18 segments, whereas GCS was computed using a 6-segment model. End-systolic GLS and GCS

were computed at the time of aortic valve closure, as previously described (12).

In addition to these ejection phase indexes, end-systolic meridional wall stress (ESWS) was calculated using the following equation:

$$\text{ESWS} = (1.33 \times \text{LVESP} \times \text{LVESD})/(4 \times \text{ESPWTh}\,[1 + (\text{ESPWTh}/\text{LVESD})])$$

where LVESP is the LV end-systolic pressure, LVESD is the LV end-systolic diameter, and ESPWTh is the end-systolic posterior wall thickness. For the calculation of ESWS, LVESP was considered to be equal to mean arterial pressure, and the echocardiographic measurements were made at end-systole. We also calculated ESWS using left ventricular peak systolic pressure (LVPSP) (13). In normal control subjects, LVPSP was estimated by systolic cuff pressure, and, in patients with AS, by adding the mean pressure gradient to the systolic cuff pressure.

MORPHOLOGICAL TISSUE ANALYSIS. At the time of AVR, 2 to 4 transmural myocardial biopsies, weighing approximately 25 to 75 mg each, were harvested from the anterior wall, between the first and second diagonal branches using a Tru-Cut biopsy needle (CareFusion, Waukegan, Illinois), as previously described (14). Samples were immediately fixed in 10% buffered formalin, embedded in paraffin, sectioned, and stained with picrosirius red (15). Stained sections were digitized with a SCN400 slide scanner (Leica Biosystems, Wetzlar, Germany). Quantification was performed using TissueIA software (Leica Biosystems, Dublin, Ireland). After elimination of artifacts and peri-vascular fibrosis, the area occupied by interstitial fibrosis was expressed as a proportion of the total myocardial area. Four different histological slices were analyzed per patient.

STATISTICAL ANALYSIS. All analyses were performed using SPSS (IBM, Armonk, New York) and the Stata (Stata, College Station, Texas) software. Continuous variables were expressed as mean ± 1 SD and categorical variables as counts and proportions. Data were tested for normality using the Kolmogorov-Smirnov test (see Supplemental Table 1) and compared using Student's *t*-tests (paired or unpaired) or the chi-square test, when appropriate. All tests were 2-sided, and p values <0.05 were considered a statistically significant difference. End-systolic stress–strain relationships were constructed by plotting GLS or GSC against ESWS in both healthy control subjects and patients with severe AS (16). The relationships obtained in healthy control subjects were fitted to a simple linear regression. The regression lines and their 95% confidence intervals were used to

TABLE 1 Baseline Demographic and Clinical Characteristics

	Healthy Control Subjects (n = 75)	Severe AS (n = 101)	p Value
Demographic data			
Age, yrs	56 ± 19	71 ± 10	<0.001
Male	40 (53)	57 (57)	0.296
Body surface area, kg/m^2	1.82 ± 0.18	1.89 ± 0.21	0.013
Risk factors			
Systemic hypertension	18 (24)	64 (63)	<0.001
Dyslipidemia	45 (60)	60 (59)	0.834
Diabetes	0 (0)	15 (15)	<0.001
Smokers	9 (12)	44 (44)	<0.001
Family history of coronary artery disease	9 (12)	30 (30)	0.008
Comorbidities			
Coronary artery disease	0 (0)	19 (19)	-
Stroke	0 (0)	3 (4)	
COPD	0 (0)	8 (8)	-
Atrial fibrillation	0 (0)	7 (7)	-
GFR, ml/min	119 ± 20	74 ± 18	<0.001
Symptoms			
NYHA functional class III to IV	0 (0)	14 (14)	-
Angina	0 (0)	17 (17)	-
Syncope	0 (0)	4 (4)	-

Values are mean ± SD or n (%).

COPD = chronic obstructive pulmonary disease; GFR = glomerular filtration rate; NYHA = New York Heart Association.

TABLE 2 Baseline Hemodynamic and Echocardiographic Characteristics

	Healthy Control Subjects (n = 75)	Severe AS (n = 101)	p Value
Hemodynamic date			
Heart rate, beats/min	67 ± 10	71 ± 13	0.021
Mean arterial pressure, mm Hg	98 ± 12	95 ± 13	0.128
LV function			
Indexed LVEDV, ml/m^2	68 ± 12	66 ± 16	0.492
Indexed LV mass, g/m^2	67 ± 15	90 ± 25	<0.001
LVEF, %	63 ± 5	59 ± 9	<0.001
Global longitudinal strain, %	−20 ± 2	−17 ± 2	<0.001
Global longitudinal SSI	−0.01 ± 1.4	−2.9 ± 2.2	<0.001
Global circumferential strain, %	−30 ± 3	−29 ± 5	0.110
Global circumferential SSI	−0.4 ± 4.1	−1.7 ± 3.7	0.033
ESWS, 10^3 dynes/cm^2	37 ± 14	33 ± 15	0.051
Indexed stroke volume, ml/m^2	40 ± 11	38 ± 9	0.073
Sphericity index	0.57 ± 0.13	0.45 ± 0.18	<0.001
Thickness to radius ratio	0.38 ± 0.10	0.51 ± 0.14	<0.001
Aortic valve stenosis indexes			
Mean transvalvular FR, ml/s	-	225 ± 57	-
Peak velocity, cm/s	-	420 ± 69	-
Mean gradient, mm Hg	-	45 ± 15	-
EOA, cm^2	-	0.70 ± 0.16	-
Indexed EOA, cm^2/m^2	-	0.37 ± 0.08	-

Values are mean ± SD.

EOA = effective orifice area; ESWS = end-systolic wall stress, FR = flow rate; LV = left ventricular; LVEDV = left ventricular end-diastolic volume; LVEF = left ventricular ejection fraction; SSI = stress–strain index.

FIGURE 1 End-Systolic Stress–Strain Relationships in Healthy Control Subjects

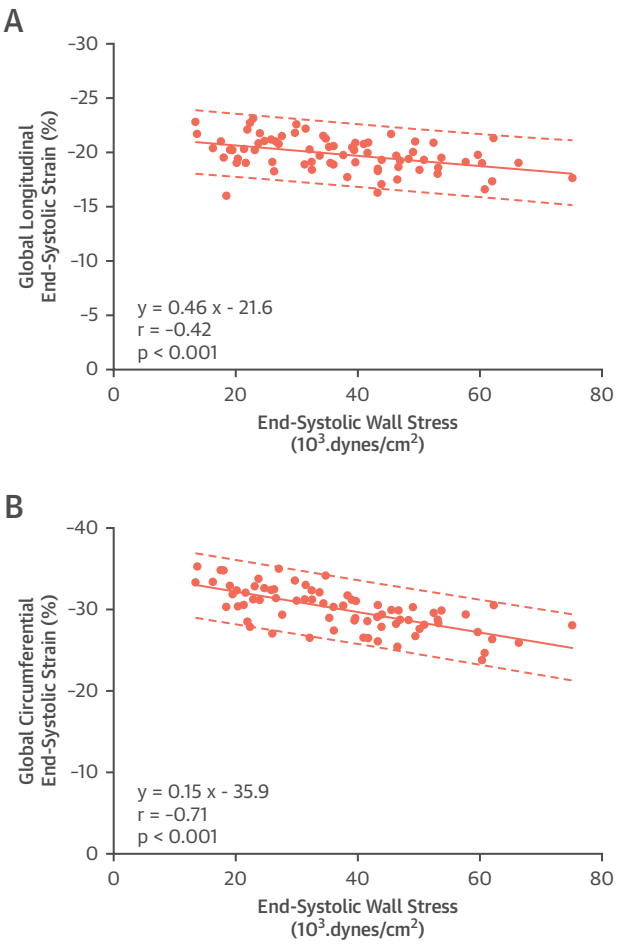

(A) Relationship between end-systolic wall stress and global longitudinal and circumferential **(B)** end-systolic strain in 75 healthy control subjects, along with 95% confidence intervals. A linear inverse correlation was observed between these parameters.

define the normal range of myocardial strains over a broad range of afterload conditions (17). To verify that the obtained end-systolic stress–strain relationships were independent of age, a similar analysis was conducted using the data from an age-matched subgroup. For this purpose, a single logistic regression score, with age as the sole variable, was generated for each healthy control subject and patient with severe AS, and used to select pairs of subjects with matched scores in the 2 groups (2:1 match) using a greedy, nearest-neighbor matching algorithm and a caliper of 0.20 SD of the logistic regression score. Individual end-systolic stress–strain data points of patients with severe AS were then plotted on the same graphs. End-systolic stress–strain indexes (the number of SDs from the mean regression line) were calculated and used as an afterload-independent index of myocardial function (Supplemental Figure 1) (17,18). Forward stepwise multiple regression analysis was used to assess potentially independent correlates of GLS, GCS, and their corresponding stress–strain indexes. Receiver-operating characteristic curve analysis was used to determine thresholds of interstitial myocardial fibrosis that were associated with depressed longitudinal or circumferential stress–strain indexes. For this purpose, the best cutoffs of interstitial myocardial fibrosis were defined as the highest Youden index. Finally, intraobserver and interobserver agreement for strain measurements was tested in 20 randomly selected cases according to the Bland-Altman method and expressed as bias (mean absolute difference ± SD) and intraclass correlation coefficients.

RESULTS

BASELINE CLINICAL, HEMODYNAMIC, AND ECHOCARDIOGRAPHIC CHARACTERISTICS. The clinical, demographic, and echocardiographic characteristics of the study population are shown in **Tables 1 and 2**. On average, healthy volunteers were younger and presented with fewer cardiovascular risk factors and comorbidities than patients with severe AS.

From an echocardiographic point of view, LVEF was higher and GLS was lower in healthy control subjects than in patients with severe AS. In contrast, ESWS tended to be lower in patients with severe AS than that in healthy control subjects, but not significantly.

END-SYSTOLIC STRESS–STRAIN RELATIONSHIPS IN HEALTHY CONTROL SUBJECTS. The relationship between ESWS and either GLS or GCS in healthy control subjects is shown in **Figure 1**. As expected, a significant inverse correlation was observed between myocardial strains and ESWS. The 95% confidence interval of these linear relations was used to define the normal range of myocardial strains over a broad range of afterload conditions. The end-systolic stress–strain relationships obtained in the age-matched subgroup (Supplemental Tables 2 and 3) were similar and not statistically different from those obtained in the entire cohort (GLS = [0.056 × ESWS] − 21.8; SEE = 1.4 in matched healthy control subjects vs. GLS = [0.046 × ESWS] − 21.6; SEE = 1.5 in the entire cohort; GCS = [0.133 × ESWS] − 35.3; SEE = 2.0 in matched healthy control subjects vs. GCS = [0.148 × ESWS] − 35.9; SEE = 2.2 in the entire cohort).

END-SYSTOLIC STRESS–STRAIN RELATIONSHIPS IN PATIENTS WITH SEVERE AS. Figure 2 shows the distribution of end-systolic stress–strain data points of individual patients with severe AS. As illustrated, myocardial strains were also afterload-dependent in patients with severe AS. However, their end-systolic stress–strain relationships differed from that in healthy control subjects. For GCS, although all but 18 end-systolic stress–strain data points were found to be within 2 SDs of normal, the slope of the end-systolic stress–strain relationship was significantly steeper than that in heathy control subjects ($p = 0.021$ for the difference in slopes; $p = 0.55$ for the difference in intercepts). For GLS, a significant parallel downward shift of the end-systolic stress–strain relationship was observed ($p = 0.21$ for the difference in slopes; $p = 0.005$ for the difference in intercepts), with approximately one-half the individual end-systolic stress–strain data points being below 2 SDs of normal (Central Illustration). Similar results were obtained if LVPSP was used in the ESWS equation (Supplemental Figure 2).

As shown in Table 3, patients whose end-systolic stress–strain data points were below 2 SDs of normal were more likely to be in atrial fibrillation, to exhibit a higher LV mass and a lower EF, and to display a higher degree of interstitial myocardial fibrosis.

MULTIVARIATE DETERMINANTS OF GLS, GCS, AND END-SYSTOLIC STRESS–STRAIN INDEXES IN PATIENTS WITH SEVERE AS. As shown in Table 4, stepwise multiple regression analysis identified the degree of interstitial fibrosis, ESWS, and atrial fibrillation as independent correlates of both pre-operative GLS and GCS. Multivariate analysis also identified interstitial fibrosis and atrial fibrillation as the only significant correlates of pre-operative longitudinal and circumferential end-systolic stress–strain indexes (Supplemental Table 4, Figure 3). Similar results were obtained if LVPSP was used in the ESWS equation (Supplemental Tables 5 and 6). Figure 4 illustrates representative strain curves and histological cross-sections from 2 patients with normal and reduced longitudinal end-systolic stress–strain indexes.

THRESHOLDS OF INTERSTITIAL MYOCARDIAL FIBROSIS ASSOCIATED WITH DEPRESSED STRESS–STRAIN INDEXES. Receiver-operating characteristics curve analysis was used to identify the cutoff values of interstitial myocardial fibrosis associated with reduced longitudinal or circumferential stress–strain indexes. For both stress–strain indexes, a cutoff value of 4.88% was indentified (AUC: 0.73 for longitudinal stress–strain indexes and 0.76 for circumferential stress–strain indexes).

FIGURE 2 End-Systolic Stress–Strain Relationships in Patients With Severe AS

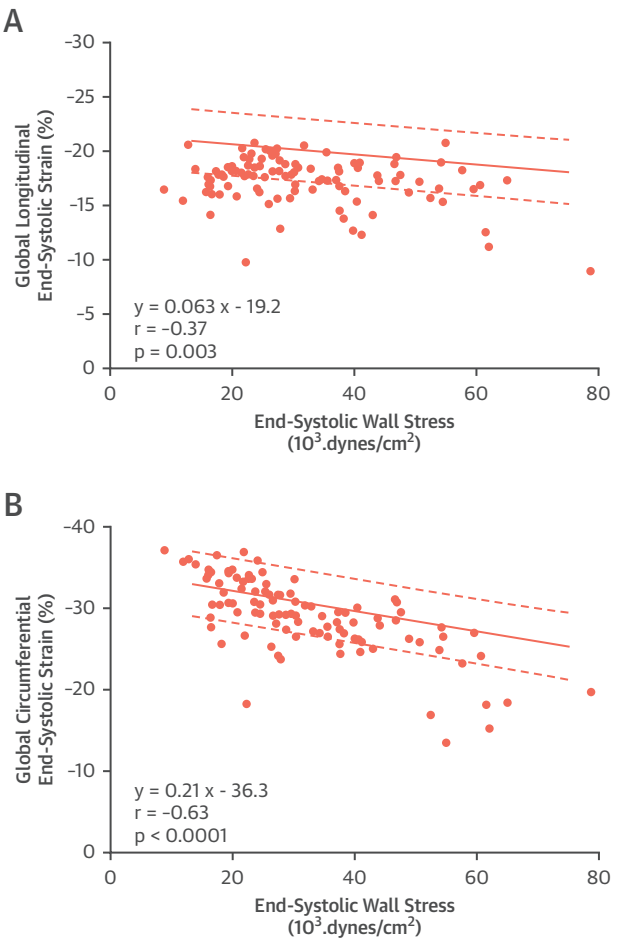

Relationship between end-systolic wall stress and global longitudinal **(A)** and circumferential **(B)** end-systolic strain in 101 patients with severe aortic stenosis (AS), along with 95% confidence intervals of the same relationship in healthy control subjects.

PRE-OPERATIVE CORRELATES OF POST-OPERATIVE LONGITUDINAL AND CIRCUMFERENTIAL FUNCTION. Changes in hemodynamic and echocardiographic parameters after AVR are shown in Table 5. GLS improved 6 months after surgery, whereas LVEF and GCS did not. Stepwise multivariate regression analysis identified pre-operative end-systolic stress–strain indexes as the only independent correlates of both post-operative longitudinal and circumferential end-systolic stress–strain indexes (ß = 0.49 and ß = 0.60, respectively; both $p < 0.001$).

CENTRAL ILLUSTRATION **End-Systolic Stress–Strain Relationship in Severe AS and its Relationship to Interstitial Myocardial Fibrosis**

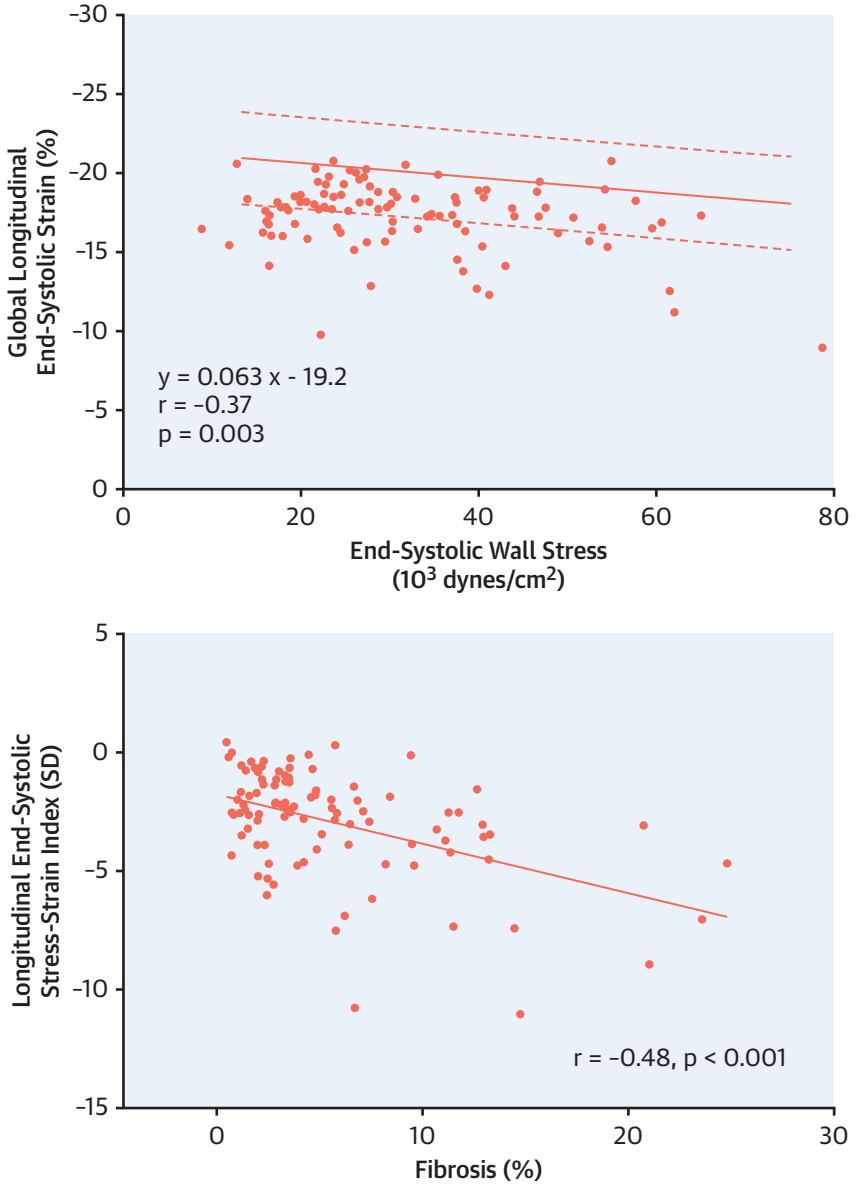

Slimani, A. et al. J Am Coll Cardiol Img. 2019;■(■):■–■.

(Top) Relationship between end-systolic wall stress and global longitudinal end-systolic strain in 101 patients with severe aortic stenosis (AS), along with 95% confidence intervals of the same relationship in healthy control subjects. **(Bottom)** Scatterplot comparing global longitudinal end-systolic stress–strain indexes and the extent of interstitial myocardial fibrosis on histology. An inverse correlation was found between these parameters, indicating lesser contractility in the presence of higher amounts of interstitial fibrosis.

Empirical receiver-operating characteristic curves were also generated to determine the optimal cutoff values of pre-operative longitudinal and circumferential end-systolic stress–strain indexes for prediction of persistent post-operative dysfunction. By using a cutoff value of −3 SDs for longitudinal end-systolic stress–strain index (AUC: 0.76) and −4 SDs for circumferential end-systolic stress–strain index

TABLE 3 Baseline Hemodynamic and Echocardiographic Characteristics According to SSIs

	LSSI >−2 SD (n = 60)	LSSI <−2 SD (n = 41)	p Value	CSSI >−2 SD (n = 83)	CSSI <−2 SD (n = 18)	p Value
Clinical data						
Atrial fibrillation	2 (3)	5 (13)	0.097	1 (1)	6 (33)	<0.001
Hemodynamic data						
Heart rate, beats/min	69 ± 10	75± 16	0.031	70 ± 12	80 ± 16	0.003
Mean arterial pressure, mm Hg	96 ± 13	94 ± 12	0.371	95 ± 13	96 ± 14	0.856
LV function						
Indexed LVEDV, ml/m^2	65 ± 13	68 ± 20	0.471	65 ± 15	72 ± 20	0.121
Indexed LV mass, g/m^2	83 ± 22	100 ± 27	0.001	87 ± 24	104 ± 28	0,009
LVEF, %	61 ± 7	57 ± 9	0.006	61 ± 7	54 ± 11	0.001
LVEF <50%	1 (2)	5 (12)	0.013	1 (1)	5 (5)	<0.001
ESWS, 10^3 dynes/cm^2	33 ± 12	32 ± 17	0.844	31 ± 13	41 ± 17	0.004
Indexed stroke volume, ml/m^2	39 ± 9	36 ± 10	0.201	38 ± 9	34 ± 11	0.069
Sphericity index	0.45 ± 0.16	0.45 ± 0.22	0.986	0.43 ± 0.17	0.52 ± 0.23	0.068
Thickness to radius ratio	0.48 ± 0.12	0.55 ± 0.17	0.020	0.51 ± 0.14	0.52 ± 0.17	0.770
Aortic valve stenosis indexes						
Mean transvalvular FR, ml/s	224 ± 51	226 ± 64	0.819	229 ± 54	207 ± 68	0.151
Peak velocity, cm/s	419 ± 63	421 ± 77	0.862	426 ± 65	389 ± 81	0.038
Mean pressure gradient, mm Hg	45 ± 14	45 ± 17	0.931	47 ± 14	38 ± 18	0.027
EOA, cm^2	0.70 ± 0.16	0.72 ± 0.15	0.517	0.70 ± 0.16	0.71 ± 0.15	0.760
Indexed EOA, cm^2/m^2	0.38 ± 0.08	0.37 ± 0.08	0.715	0.37 ± 0.08	0.38 ± 0.08	0.777
Histology						
Interstitial fibrosis, %	3.8 ± 2.9	8.3 ± 6.3	<0.001	4.9 ± 4.4	9.5 ± 6.4	0.001

Values are n (%) or mean ± SD.
CSSI = circumferential stress–strain index; LSSI = stress–strain index; other abbreviation as in Table 2.

(AUC: 0.84), persistent post-operative dysfunction was identified with a sensitivity of 82% and 80%, respectively, and a specificity of 76% and 72%.

REPRODUCIBILITY. Intraobserver and interobserver reproducibility was evaluated in 20 randomly selected patients. Results are shown in Table 6.

DISCUSSION

The aim of the present study was to investigate the respective contribution of excessive afterload and interstitial fibrosis to the pre- and post-operative LV systolic strain in patients with severe AS and to test whether pre-operative end-systolic stress–strain relationships can be used to identify patients with persistent LV dysfunction after AVR. Our results can be summarized as follows.

1) In healthy control subjects, both GLS and GCS displayed significant dependence on afterload.
2) In patients with severe AS, GLS and GCS strains also displayed significant afterload dependence. Longitudinal end-systolic stress–strain relationships were significantly shifted downward compared with healthy control subjects, which suggested reduced myocardial longitudinal contractile function.
3) Patients with reduced pre-operative longitudinal and circumferential end-systolic stress–strain indexes exhibited larger degrees of interstitial myocardial fibrosis than patients without.
4) By multivariate analysis, pre-operative stress–strain indexes were found to be the only significant predictors of post-operative stress–strain indexes.

LOAD-DEPENDENCE OF LV EJECTION PHASE INDEXES. Despite decades of experimental and clinical research, assessing LV contractile performance remains a complex and difficult task. In daily clinical practice, this is usually achieved by calculating the LVEF or the percent fractional shortening (12). However, these ejection phase indexes are markedly affected by the heart's loading conditions and vary directly with end-diastolic fiber length (pre-load) and inversely with afterload (4,19). Their clinical usefulness is thus limited by their inability to distinguish between the mechanical effects of altered loading conditions and an intrinsic depression of the inotropic state.

TABLE 4 Univariate and Multivariate Determinants of Pre-Operative Longitudinal and Circumferential Strains

	Univariate Analysis		Multivariate Analysis	
	R	p Value	ß	p Value
Global longitudinal strain				
Interstitial fibrosis	0.50	<0.001	0.35	<0.001
LV ejection fraction	−0.45	<0.001		
ESWS	0.42	<0.001	0.25	0.005
Atrial fibrillation	0.41	<0.001	0.26	0.003
Indexed LV mass	0.41	<0.001		
Indexed stroke volume	−0.33	0.001		
Indexed LVEDV	0.25	0.013		
Sphericity index	0.22	0.025		
Mean pressure gradient	−0.21	0.037		
Peak transaortic velocity	−0.20	0.043		
Mean flow rate	−0.19	0.063		
Global circumferential strain				
ESWS	0.65	<0.001	0.51	<0.001
LV ejection fraction	−0.51	<0.001		
Atrial fibrillation	0.51	<0.001	0.35	<0.001
Interstitial fibrosis	0.45	<0.001	0.19	0.010
Sphericity index	0.43	<0.001		
Indexed stroke volume	−0.38	<0.001		
Indexed LV mass	0.34	0.001		
Indexed LVEDV	0.29	0.003		
Peak transaortic velocity	−0.28	0.005		
Mean flow rate	−0.27	0.006		
Mean pressure gradient	−0.27	0.006		
Thickness to radius ratio	−0.18	0.073		

Abbreviations as in Table 2.

Several alternative methods for assessing LV contractile performance have been proposed to overcome these limitations. It has been known for many years that the LV isovolumetric force–length relation, which is dependent on contractile state, describes the maximal force attainable for any degree of myocardial stretch (20,21). Experimental data have shown that LV force–length relations obtained either during isovolumetric contractions or at the end of ejection in isotonically contracting hearts are virtually identical (22,23). For any LV contractile state, the LV isovolumetric force–length relation predicts that shortening of isotonic contractions will cease when the active force–length relation coincides with a point on the isovolumetric force–length line. At this point, the LV wall force equals the maximal force that muscle length can sustain, and LV shortening ends. This relation was shown to be sensitive to the contractile state, to be independent of end-diastolic fiber length and peak LV ejection forces, and to incorporate afterload (24). These studies of basic cardiovascular physiology provide the rationale for using ESWS (i.e., the force opposing shortening or afterload) and shortening relationships as an index of the contractile state that incorporates afterload. These relationships have been extensively validated in humans and successfully used in various physiological and pathological conditions (16–18)

DEVELOPMENT OF ESWS–MYOCARDIAL STRAIN RELATIONS. In recent years, myocardial deformation indexes, such as GLS, GCS, and radial strain, were proposed as an alternative to conventional ejection phase indexes (12). These indexes, and particularly those derived from 2-dimensional speckle tracking echocardiography, were extensively validated. They were also shown to be highly reproducible and to offer incremental prognostic information over LVEF in a variety of cardiac conditions (25). Similar to conventional LV ejection phase indexes, myocardial strains are nonetheless influenced by the heart's loading conditions (26). It thus mandatory to take the prevailing loading conditions into consideration when interpreting myocardial strain measurements.

In the present study, we constructed ESWS–myocardial strain relationships by plotting GLS or GSC against ESWS in both healthy control subjects and patients with severe AS (16–18). The relationships obtained in normal control subjects were fitted to a simple linear regression model and used to define the normal range of myocardial strains over a broad range of afterload conditions, as previously validated (16). Individual stress–strain data points of patients with severe AS were then plotted on the same graph. The vertical distance of each individual patient data point with respect to the normal regression line was used as an afterload-independent index of myocardial performance. Our data confirmed that myocardial strains are afterload-dependent, both in normal individuals and in patients with severe AS. Interestingly, in patients with severe AS, the end-systolic stress–strain relationships differed from that in healthy control subjects. For GCS, most end-systolic stress–strain data points were found within 2 SDs of normal. However, the slope of the end-systolic stress–strain relationship was significantly steeper than that in healthy control subjects. For GLS, a significant parallel downward shift of the end-systolic stress–strain relationship was observed, with approximately one-half the individual end-systolic stress–strain data points being found below 2 SDs of normal. These data suggested that the longitudinal function became depressed before the circumferential function did. Similar results, that is, reduced longitudinal function despite normal EF and GCS, were reported by other investigators, and were found to correlate with more extensive LV

remodeling (higher LV mass and presence of concentric LV hypertrophy) and greater severity of AS (27-29) Surprisingly, none of these studies attempted to take afterload into consideration. When adjusting for afterload using end-systolic stress–strain relationships, only one-half of our patients with severe AS presented with truly depressed longitudinal function. More importantly, only 2 parameters were found to correlate with reduced end-systolic stress–strain indexes, namely, tissue fibrosis and atrial fibrillation.

INTERSTITIAL MYOCARDIAL FIBROSIS IN SEVERE AS. The association between LV hypertrophy and the development of interstitial myocardial fibrosis in patients with severe AS has been known for many years. Back in the early 1980s, Krayenbuehl et al. (8) demonstrated that patients with severe aortic disease developed proportionate LV hypertrophy and myocardial fibrosis. These same investigators subsequently found that interstitial myocardial fibrosis directly affected LV systolic and diastolic properties and regressed more slowly after AVR than LV mass. Recently, several investigators made similar observations (30-32). These investigators also demonstrated that the presence of histological myocardial fibrosis correlated well with that of mid-wall late gadolinium enhancement on cardiac magnetic resonance studies. They also showed that the presence and extent of these mid-wall late enhancement areas was associated with poorer post-operative outcome.

In the present study, we examined the impact of interstitial myocardial fibrosis on GLS and GCS using end-systolic stress–strain relationships to adjust for the confounding effects of afterload. We found that whenever the end-systolic stress–strain indexes were <2 SDs of normal, this was associated with larger amounts of interstitial myocardial fibrosis as determined by histology.

FIGURE 3 Relation of End-Systolic Stress–Strain Indexes to Interstitial Myocardial Fibrosis

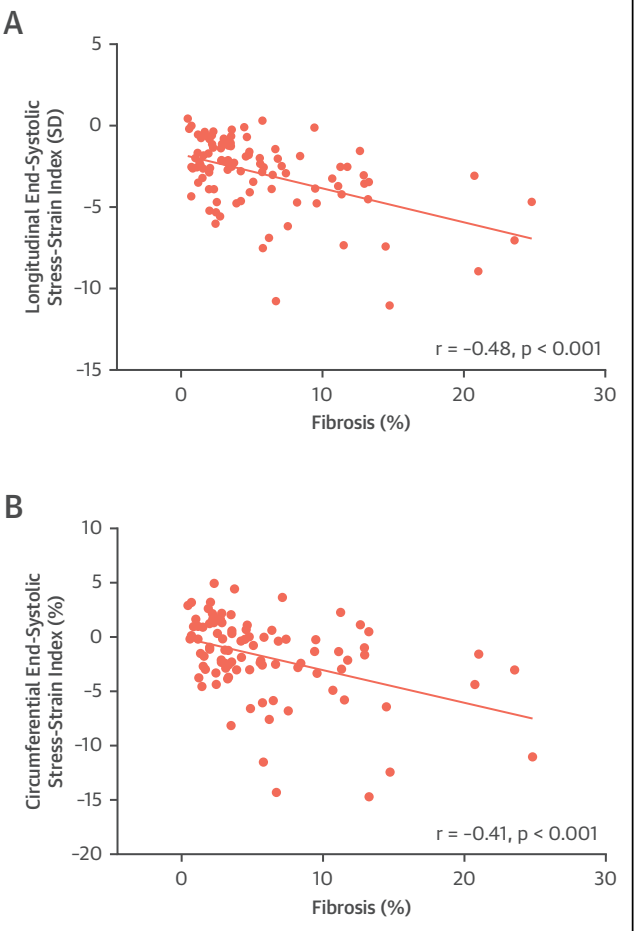

Scatterplot comparing **(A)** global longitudinal and **(B)** circumferential end-systolic stress–strain indexes and the extent of interstitial myocardial fibrosis on histology. An inverse correlation was found between these parameters, indicating lesser contractility in the presence of higher amounts of interstitial fibrosis.

ATRIAL FIBRILLATION AND MYOCARDIAL DEFORMATION IN SEVERE AS. Another salient finding of our study was the association between atrial fibrillation and depressed longitudinal function in patients with severe AS. Although speculative, we believe this was due to the reduced pre-load that accompanies atrial fibrillation. We and others (4,5,33) demonstrated that patients with severe AS were extremely dependent on atrial contraction to maintain stroke volume and cardiac output within normal limits. We also demonstrated that patients with severe AS and LV hypertrophy frequently displayed markedly prolonged relaxation constants, making their diastolic filling volume, and hence, their forward stroke volume, extremely dependent on the duration of diastole (33). In atrial fibrillation, both phenomena (i.e., the loss of atrial contribution to LV filling and the reduced diastolic filling time) contribute to reducing the filling volume, and subsequently, the forward stroke volume. Combined with the loss of pre-load reserve that characterizes pressure-overloaded LVs, the onset of atrial fibrillation is thus likely to result in reduced pre-load and aggravation of afterload mismatch, and hence, in altered ejection phase indexes, such as LVEF and myocardial strain.

CLINICAL IMPLICATIONS. Our findings have important clinical implications. First, they demonstrate that the presence of truly depressed longitudinal or

FIGURE 4 Changes in Myocardial Strain After AVR

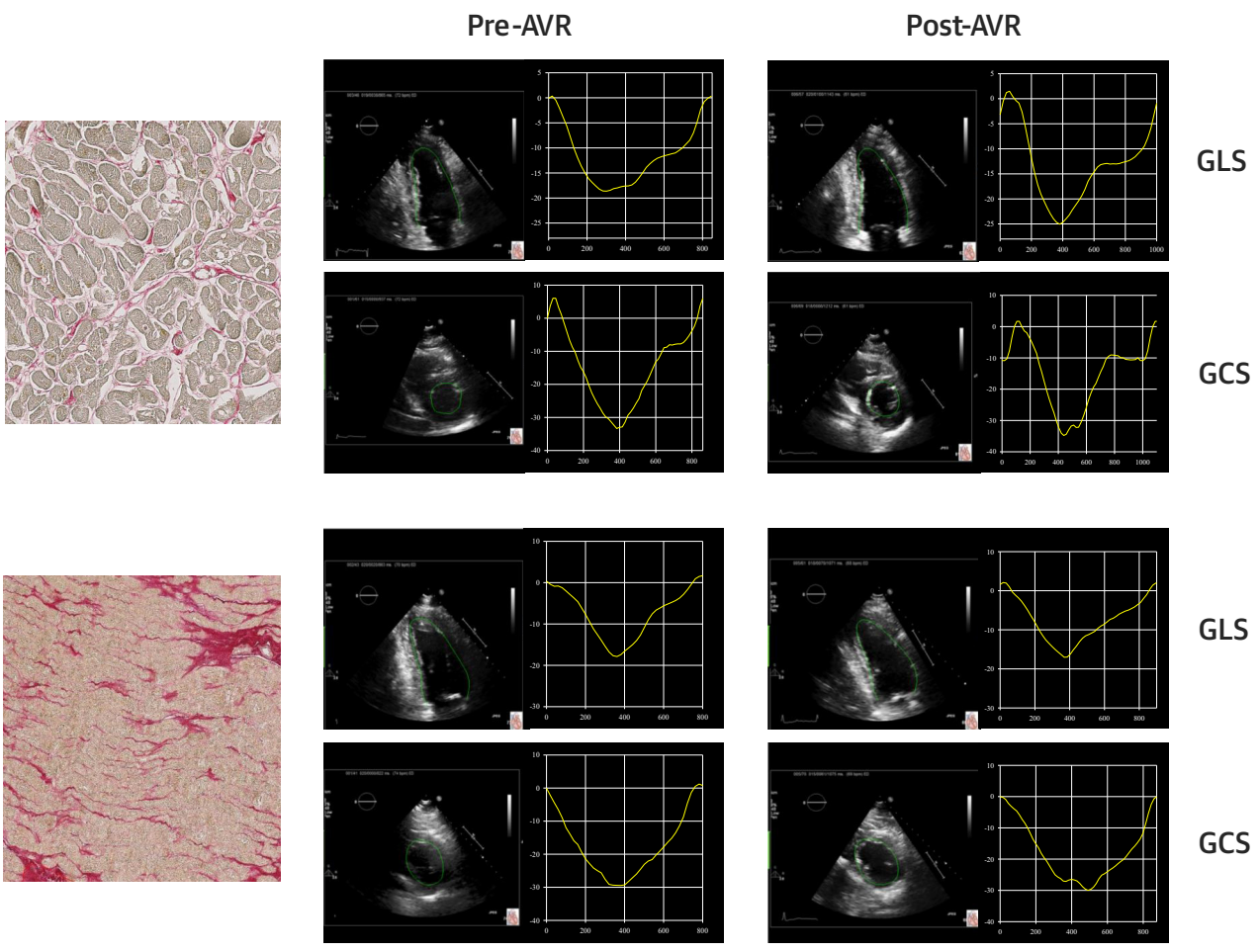

Representative examples of 2 patients with severe AS (aortic valve area [AVA] 1 cm^2 and indexed AVA 0.6 cm^2/m^2). Both display reduced pre-operative global longitudinal strain (GLS). The patient in the **top panel** had a low degree of interstitial fibrosis (0.7%) and recovered normal longitudinal function post-operatively, whereas the patient in the **bottom panel** exhibited larger degrees of interstitial fibrosis (12.9%) and displayed no significant recovery of longitudinal function post-operatively. AVR = aortic valve replacement; GCS = global circumferential strain; other abbreviation as in Figure 2.

circumferential function, as identified by end-systolic stress–strain relationships, is a marker of significant myocardial tissue damage. Second, they allow predicting which patient is unlikely to recover normal systolic function after AVR. We found a strong association between end-systolic stress–strain indexes measured 6 months after AVR and both interstitial myocardial fibrosis and pre-operative end-systolic stress–strain indexes. We also found that these indexes allowed predicting persistent post-operative dysfunction with a sensitivity of 80% to 82% and a specificity of 72% to 76%. Few previous studies have investigated the ability of myocardial deformation indexes to predict functional recovery or LV reverse remodeling after AVR (34-36) Although these studies demonstrated that pre-operative myocardial strain was a predictor of post-operative functional recovery, the published cutoff values were quite varied, probably due to the known vendor dependency of normal strain values (37). In this regard, the present approach might offer a vendor-independent solution, with stress–strain indexes being expressed in relative terms rather than in absolute terms.

STUDY LIMITATIONS. This study had limitations that should be acknowledged. First, we used the mean arterial pressure as a surrogate to end-systolic arterial

TABLE 5 Changes in Hemodynamic and Echocardiographic Parameters After AVR

	Pre-Op	Post-Op	p Value
Hemodynamic date			
Heart rate, beats/min	71 ± 13	70 ± 13	0.525
Mean arterial pressure, mm Hg	95 ± 13	96 ± 11	0.179
LV function			
Indexed LVEDV, ml/m^2	66 ± 16	71 ± 17	0.061
Indexed LV mass, g/m^2	90 ± 25	76 ± 16	<0.001
LV ejection fraction, %	59 ± 9	60 ± 8	0.559
Global longitudinal strain, %	−17 ± 2	−18 ± 3	0.001
Global longitudinal SSI	−2.9 ± 2.2	−1.8 ± 2.8	<0.001
Global circumferential strain, %	−29 ± 5	−30 ± 5	0.378
Global circumferential SSI	−1.7 ± 3.7	−1.1 ± 4.3	0.100
ESWS, 10^3 dynes/cm^2	33 ± 15	33 ± 13	0.240
Sphericity index	0.45 ± 0.18	0.42 ± 0.13	0.281
Thickness to radius ratio	0.51 ± 0.14	0.51 ± 0.12	0.996
Aortic valve stenosis indexes			
Mean transvalvular FR, ml/s	225 ± 57	230 ± 71	0.894
Peak velocity, cm/s	420 ± 69	193 ± 54	<0.001
Mean gradient, mm Hg	45 ± 15	9 ± 5	<0.001
EOA, cm^2	0.72 ± 0.16	1.86 ± 0.70	<0.001
Indexed EOA, cm^2/m^2	0.37 ± 0.08	0.98 ± 0.36	<0.001

Values are mean ± SD.
AVR = aortic valve replacement; other abbreviations as in Table 2.

TABLE 6 Intraobserver and Interobserver Reproducibility

	Intraobserver Reproducibility			Interobserver Reproducibility		
	ICC	95% CI	Bias	ICC	95% CI	Bias
Global longitudinal strain	0.87	0.72–0.96	0.02 ± 0.59	0.84	0.58–0.94	0.04 ± 0.95
Global circumferential strain	0.89	0.74–0.96	0.03 ± 1.43	0.86	0.61–0.96	0.20 ± 1.40

CI = confidence interval; ICC = intraclass correlation coefficient.

pressure instead of calculating this parameter by calibrated carotid pulse tracings (38), as was done in our previous studies (18,33). This was due to the unavailability of the appropriate instrument on the echocardiographic systems used in this study. Nonetheless, based on the high degree of covariance between mean arterial pressure and end-systolic arterial pressure that we found in our previous experience ($r^2 = 0.89$; $p < 0.001$) (Supplemental Figure 3) (33), we did not believe this significantly affected our results. Second, the control subjects were not matched to the patients with severe AS, particularly with respect to age and cardiovascular risk factors. Arguably, this could have affected the measurements made, and thereby, could have confounded the normal ranges provided. As shown earlier, the end-systolic stress–strain relationships obtained with the data with the data of an age-matched subgroup of healthy control subjects being similar to those obtained in the whole cohort, this was unlikely the case.

CONCLUSIONS

Because of their afterload dependence, myocardial strains should be assessed together with end-systolic wall stress. This is particularly important in patients with LV hypertrophy, who had depressed contractility can be concealed by the increase in wall thickness. In patients with severe AS, end-systolic stress–strain relationships allow identification of patients presenting with significant interstitial myocardial fibrosis and predict the extent of recovery of myocardial strains after AVR.

ADDRESS FOR CORRESPONDENCE: Dr. Jean-Louis Vanoverschelde, Division of Cardiology, Cliniques Universitaires Saint-Luc, Avenue Hippocrate 10-2881, B-1200 Brussels, Belgium. E-mail: jean-louis.vanoverschelde@uclouvain.be.

PERSPECTIVES

COMPETENCY IN MEDICAL KNOWLEDGE: In patients with severe AS, and particularly those with LV hypertrophy, who had depressed contractility can be concealed by the increase in wall thickness, myocardial strains should always be assessed together with ESWS. In these patients, end-systolic stress–strain relationships allow identification of patients presenting with significant interstitial myocardial fibrosis and predict the extent of recovery of myocardial strains after AVR.

TRANSLATIONAL OUTLOOK: Additional studies, preferably multicentric, are needed to validate the present findings and to test whether the results of the present study are applicable to all patients who undergo AVR for the treatment of severe AS.

REFERENCES

1. Ross J Jr. Afterload mismatch in aortic and mitral valve disease. Implications for surgical therapy. J Am Coll Cardiol 1985;5:811–26.

2. Carabello BA, Green LH, Grossman W, et al. Hemodynamic determinants of prognosis of aortic valve replacement in critical aortic stenosis and advanced congestive heart failure. Circulation 1980;62:42–8.

3. Grossman W, Jones D, McLaurin LP. Wall stress and patterns of hypertrophy in the human left ventricle. J Clin Invest 1975;56:56–64.

4. Gunther S, Grossman W. Determinants of ventricular function in pressure-overload hypertrophy in man. Circulation 1979;59:679–88.

5. Ross J Jr. Afterload mismatch and preload reserve: a conceptual framework for the analysis of ventricular function. Prog Cardiovasc Dis 1976; 18:255–64.

6. Carabello BA, Spann JF. The uses and limitations of end-systolic indexes of left ventricular function. Circulation 1984;69:1058–64.

7. Hein S, Arnon E, Kostin S, et al. Progression from compensated hypertrophy to failure in the pressure-overloaded human heart. Structural deterioration and compensatory mechanisms. Circulation 2003;107. 984–914.

8. Krayenbuehl HP, Hess OM, Monrad ES, Schneider J, Mall G, Turina M. Left ventricular myocardial structure in aortic valve disease before, intermediate, and late after aortic valve replacement. Circulation 1989;79:744–55.

9. Vahanian A, Alfieri O, Andreotti F, et al. Joint Task Force on the Management of Valvular Heart Disease of the European Society of Cardiology (ESC); European Association for Cardio-Thoracic Surgery (EACTS), Guidelines on the management of valvular heart disease (version 2012). Eur Heart J 2013;33:2451–96.

10. Baumgartner H, Hung J, Bermejo J, et al. Echocardiographic assessment of valve stenosis: EAE/ASE recommendations for clinical practice. Eur J Echocardiogr 2009;10:1–25.

11. Devereux RB, Reichek N. Echocardiographic determination of left ventricular mass in man. Anatomic validation of the method. Circulation 1977;55:613–8.

12. Lang RM, Badano LP, Mor-Avi V, et al. Recommendations for cardiac chamber quantification by echocardiography in adults: an update from the American Society of Echocardiography and the European Association of Cardiovascular Imaging. J Am Soc Echocardiogr 2015;28:1–39.

13. Douglas P, Reichek N, Plappert T, Muhammad A, St. John Sutton MG. Comparison of echocardiographic methods for assessment of left ventricular shortening and wall stress. J Am Coll Cardiol 1987;9:945–51.

14. de Meester de Ravenstein C, Bouzin C, Lazam S, et al. Histological validation of measurement of diffuse interstitial myocardial fibrosis by myocardial extravascular volume fraction from Modified Look-Locker imaging (MOLLI) T1 mapping at 3 T. J Cardiovasc Magn Reson 2015;17:48.

15. Whittaker P, Kloner RA, Boughner DR, Pickering JG. Quantitative assessment of myocardial collagen with picrosirius red staining and circularly polarized light. Basic Res Cardiol 1994; 89:397–410.

16. Borow KM, Green LH, Grossman W, Braunwald E. Left ventricular end-systolic stress-shortening and stress-length relations in humans. Normal values and sensitivity to inotropic state. Am J Cardiol 1982;50:1301–8.

17. Colan SD, Borow KM, Neumann A. Left ventricular end-systolic wall stress-velocity of fiber shortening relation. A load-independent index of myocardial contractility. J Am Coll Cardiol 1984;4: 715–24.

18. Vanoverschelde J-L, Younis L, Melin JA, et al. Prolonged exercise induces left ventricular dysfunction in healthy subjects. J Appl Physiol 1991;70:1356–63.

19. Weber KT, Janicki JS, Reeves RC, Hefner LL. Factors influencing left ventricular shortening in isolated canine heart. Am J Physiol 1976;230: 419–26.

20. Holt JP. Regulation of the degree of emptying of the left ventricle by the force of ventricular contraction. Circ Res 1957;5:281–7.

21. Weber KT, Janicki JS, Hefner LL. Left ventricular force-length relations of isovolumic and ejecting contractions. Am J Physiol 1976;231: 337–43.

22. Downing SE, Sonneblick EH. Cardiac muscle mechanics and ventricular performance. Am J Physiol 1964;207:705–15.

23. Suga H, Sagawa K. Instantaneous pressure-volume relationships and their ratio in excised, supported canine left ventricle. Circ Res 1974;35: 117–26.

24. Grossman W, Braunwald E, Mann T, McLaurin LP, Green LH. Contractile state of the left ventricle in man as evaluated from the end-systolic pressure-volume relation. Circulation 1977;56:845–52.

25. Yotti R, Bermejo J, Benito Y, et al. Validation of noninvasive indices of global systolic function in patients with normal and abnormal loading conditions. A simultaneous echocardiography pressure-volume catheterization study. Circ Cardiovasc Imaging 2014;7:164–72.

26. Collier P, Phelan D, Klein A. A test in context: myocardial strain measured by speckle-tracking echocardiography. J Am Coll Cardiol 2017;69: 1043–56.

27. Carasso S, Cohen O, Mutlak D, et al. Differential effects of afterload on left ventricular long- and short-axis function: insights from a clinical model of patients with aortic valve stenosis undergoing aortic valve replacement. Am Heart J 2009;158:540–5.

28. Donal E, Thebault C, O'Connor K, et al. Impact of aortic stenosis on longitudinal myocardial deformation during exercise. Eur J Echocardiogr 2011;12:235–41.

29. Lafitte S, Perlant M, Reant P, et al. Impact of impaired myocardial deformations on exercise tolerance and prognosis in patients with asymptomatic aortic stenosis. Eur J Echocardiogr 2009; 10:414–9.

30. Azevedo CF, Nigri M, Higuchi ML, et al. Prognostic significance of myocardial fibrosis quantification by histopathology and magnetic resonance imaging in patients with severe aortic valve disease. J Am Coll Cardiol 2010;56:278–87.

31. Dweck MR, Joshi S, Murigu T, et al. Midwall fibrosis is an independent predictor of mortality in patients with aortic stenosis. J Am Coll Cardiol 2011;58:1271–9.

32. Chin CWL, Everett RJ, Kwiecinski J, et al. Myocardial fibrosis and cardiac decompensation in aortic stenosis. J Am Coll Cardiol Img 2017;10: 1320–33.

33. Vanoverschelde J-L, Essamri B, Michel X, et al. Hemodynamic and volume correlates of left ventricular diastolic relaxation and filling in patients with aortic stenosis. J Am Coll Cardiol 1992;20: 813–21.

34. Kempny A, Diller GP, Kaleschke G, et al. Longitudinal left ventricular 2D strain is superior to ejection fraction in predicting myocardial recovery and symptomatic improvement after aortic valve implantation. Int J Cardiol 2013;167:2239–43.

35. Staron A, Bansal M, Kalakoti P, et al. Speckle tracking echocardiography derived 2-dimensional myocardial strain predicts left ventricular function and mass regression in aortic stenosis patients undergoing aortic valve replacement. Int J Cardiovasc Imaging 2013;29:797–808.

36. Gelsomino S, Luca F, Parise O, et al. Longitudinal strain predicts left ventricular mass regression after aortic valve replacement for severe aortic stenosis and preserved left ventricular function. Heart Vessels 2013;28:775–84.

37. Farsalinos KE, Daraban AM, Ünlü S, Thomas JD, Badano LP, Voigt J-U. Head-to-head comparison of global longitudinal strain measurements among nine different vendors: the EACVI/ASE Inter-Vendor Comparison Study. J Am Soc Echocardiogr 2015;28:1171–81.

38. Colan SD, Borow KM, Neumann A. Use of the calibrated carotid pulse tracing for calculation of left ventricular pressure and wall stress throughout ejection. Am Heart J 1985;109: 1306–10.

KEY WORDS aortic stenosis, fibrosis, myocardial strain

APPENDIX For supplemental figures and tables, please see the online version of this paper.